

**NASA  
Technical  
Memorandum**

NASA TM - 108383

**A COMPARISON OF CHROMIC ACID AND SULFURIC  
ACID ANODIZING**

By M.D. Danford

Materials and Processes Laboratory  
Science and Engineering Directorate

November 1992

(NASA-TM-108383) A COMPARISON OF  
CHROMIC ACID AND SULFURIC ACID  
ANODIZING (NASA) 18 p

N93-13378

Unclass

G3/26 0131940



National Aeronautics and  
Space Administration

George C. Marshall Space Flight Center



# REPORT DOCUMENTATION PAGE

Form Approved  
OMB No. 0704-0188

Public reporting burden for this collection of information is estimated to average 1 hour per response, including the time for reviewing instructions, searching existing data sources, gathering and maintaining the data needed, and completing and reviewing the collection of information. Send comments regarding this burden estimate or any other aspect of this collection of information, including suggestions for reducing this burden, to Washington Headquarters Services, Directorate for Information Operations and Reports, 1215 Jefferson Davis Highway, Suite 1204, Arlington, VA 22202-4302, and to the Office of Management and Budget, Paperwork Reduction Project (0704-0188), Washington, DC 20503.

1. AGENCY USE ONLY (Leave blank)		2. REPORT DATE November 1992	3. REPORT TYPE AND DATES COVERED Technical Memorandum	
4. TITLE AND SUBTITLE  A Comparison of Chromic Acid and Sulfuric Acid Anodizing			5. FUNDING NUMBERS	
6. AUTHOR(S)  M.D. Danford				
7. PERFORMING ORGANIZATION NAME(S) AND ADDRESS(ES)  George C. Marshall Space Flight Center Marshall Space Flight Center, Alabama 35812			8. PERFORMING ORGANIZATION REPORT NUMBER	
9. SPONSORING / MONITORING AGENCY NAME(S) AND ADDRESS(ES)  National Aeronautics and Space Administration Washington, DC 20546			10. SPONSORING / MONITORING AGENCY REPORT NUMBER  NASA TM - 108383	
11. SUPPLEMENTARY NOTES  Prepared by Materials and Processes Laboratory, Science and Engineering Directorate.				
12a. DISTRIBUTION / AVAILABILITY STATEMENT  Unclassified — Unlimited			12b. DISTRIBUTION CODE	
13. ABSTRACT (Maximum 200 words)  Because of federal and state mandates restricting the use of hexavalent chromium, it was deemed worthwhile to compare the corrosion protection afforded 2219-T87 aluminum alloy by both Type I chromic acid and Type II sulfuric acid anodizing per MIL-A-8625. Corrosion measurements were made on large, flat 2219-T87 aluminum alloy sheet material with an area of 1 cm <sup>2</sup> exposed to a corrosive medium of 3.5-percent sodium chloride at pH 5.5. Both ac electrochemical impedance spectroscopy and the dc polarization resistance techniques were employed. The results clearly indicate that the corrosion protection obtained by Type II sulfuric acid anodizing is superior, and no problems should result by substituting Type II sulfuric acid anodizing for Type I chromic acid anodizing.				
14. SUBJECT TERMS Electrochemical Corrosion Measurements, Electrochemical Impedance Spectroscopy, Comparison of Type I and Type II Anodizing, The Polarization Resistance Technique			15. NUMBER OF PAGES 18	
			16. PRICE CODE NTIS	
17. SECURITY CLASSIFICATION OF REPORT  Unclassified	18. SECURITY CLASSIFICATION OF THIS PAGE  Unclassified	19. SECURITY CLASSIFICATION OF ABSTRACT  Unclassified	20. LIMITATION OF ABSTRACT  Unlimited	



## TABLE OF CONTENTS

	Page
INTRODUCTION .....	1
EXPERIMENTAL METHODS .....	1
EXPERIMENTAL PROCEDURES .....	2
RESULTS AND DISCUSSION .....	3
Sulfuric Acid Anodize .....	3
Chromic Acid Anodize .....	3
Comparison of Charge Transfer Resistance, Pore Resistance, and Diffusion Coefficients .....	3
Corrosion Rates .....	4
CONCLUSION .....	4
REFERENCES .....	5

## LIST OF ILLUSTRATIONS

Figure	Title	Page
1.	The New EG&G-PARC Flat Cell .....	7
2.	Primary Equivalent Circuit Model for Analysis of AC Impedance Data .....	8
3.	Equivalent Circuit Model for Calculating the Warburg Coefficient .....	9
4.	$R(T)$ , $R(P)$ , and $\sigma$ -Time Curves for Sulfuric Acid Anodize .....	10
5.	$R(F)$ , $R(S)$ , and $I_{CORR}$ -Time Curves for Sulfuric Acid Anodize .....	11
6.	$R(T)$ , $R(P)$ , and $\sigma$ -Time Curves for Chromic Acid Anodize .....	12
7.	$R(F)$ , $R(S)$ , and $I_{CORR}$ -Time Curves for Chromic Acid Anodize .....	13

## LIST OF TABLES

Table	Title	Page
1.	Chemistry of 2219-T87 Aluminum .....	6
2.	Comparison of Average Corrosion Rates Obtained With AC and DC Methods .....	6

## TECHNICAL MEMORANDUM

### A COMPARISON OF CHROMIC ACID AND SULFURIC ACID ANODIZING

#### INTRODUCTION

Due to the severe restrictions being placed on the use of hexavalent chromium (a prime component of chromic acid anodizing) by federal and state mandates, it was deemed worthwhile to investigate the corrosion protection afforded 2219-T87 aluminum alloy by this method and to compare it to the corrosion protection provided by sulfuric acid anodizing. Both electrochemical impedance spectroscopy (EIS), an alternating current (ac) method, and the polarization resistance technique (PR), a direct current (dc) method, were employed in this investigation.

A new type of corrosion cell was employed in this work; namely, the new flat cell developed by EG&G-PARC (Fig. 1). This cell allowed the use of large, flat sheet material specimens, 10.16 by 15.24 cm (4 by 6 in), of anodized 2219-T87 aluminum alloy, with an area of 1 cm<sup>2</sup> exposed to the medium contained in the cell. The use of large specimens allows greater control of anodizing conditions, resulting in more precise control of coating thicknesses. Anodizing procedures are developed primarily for larger specimens because they afford a distinct advantage over the use of the small 1.6-cm (5/8-in) diameter circular specimens previously employed, the advantage being the uniformity of thickness attained in the anodized coatings on the large specimens. In addition, the new flat cell reduces effects from crevice corrosion. 2219-T87 aluminum alloy, a prime candidate for construction of Space Station *Freedom*, was chosen in this investigation for that reason.

#### EXPERIMENTAL METHODS

As stated previously, both the EIS and the PR techniques were employed in this work. The equivalent circuit model used for analysis of EIS data is shown in Figure 2. The circuit model of Figure 3 was used to calculate the effect of diffusion polarization. A contribution due to the Warburg impedance, or the effect due to diffusion polarization, is given by

$$Z_W = \sigma \omega^{-\frac{1}{2}} - j \sigma \omega^{-\frac{1}{2}} \quad (1)$$

Here,  $Z_W$  is the Warburg impedance,  $\omega = 2\pi f$  ( $f$  = frequency),  $j = \sqrt{-1}$ , and  $\sigma$  is the Warburg coefficient. The value of  $\sigma$  is obtained using the model of Figure 3. The higher the value of  $\sigma$ , the less is the diffusion of the surrounding medium through the specimen coat. If the value of  $\sigma$  exceeds that of the charge transfer parameter  $R_T$ , the corrosion mechanism is diffusion controlled. An inverse correlation exists between the  $I_{\text{CORR}}$ -time curves and the  $\sigma$ -time curves, in that the greater the diffusion through the specimen coating, the greater is the corrosion rate of the specimen. The development and selection of these models has been discussed previously.<sup>1</sup>

Values for each of the circuit components in either Figure 1 or Figure 2 were treated as parameters in the nonlinear ORGLS<sup>2</sup> least-squares program, which automatically adjusted these

parameters to obtain a best fit to the observed Bode magnitude data (log impedance versus log  $\omega$ ). Corrosion currents were data (long impedance versus log  $\omega$ ). Corrosion currents were calculated from EIS data using the relation

$$I_{\text{CORR}} = \frac{(b_a) \times (b_c)}{2.303 (b_a + b_c)} \cdot \frac{1}{R_T + R_F} \quad (2)$$

where  $R_T + R_F$  is the total charge transfer resistance. Equation (2) is the Stern-Geary equation for charge transfer control.<sup>3-5</sup> Tafel constants ( $b_a$  and  $b_c$ ) were assumed to be 50 mV each. The value of 50 mV each for the Tafel constants has been found to provide excellent agreement with values of  $I_{\text{CORR}}$  obtained by the dc PR measurements.<sup>6</sup> The corrosion rate for 2219-T87 aluminum is given by

$$\text{Corrosion Rate (mpy)} = 0.44014 \times I_{\text{CORR}} \quad (3)$$

The derivation of the constant in equation (3) has been discussed.<sup>6</sup>

In the PR method, curves of potential versus current were obtained and the data were analyzed using the program POLCURR.<sup>7</sup> The theory for the PR technique has been described previously.<sup>8</sup> This method has an advantage in that values for the Tafel constants ( $b_a$  and  $b_c$ ) are obtained directly from the experimental data and are not assumed as in the case of EIS experiments. However, more mechanistic information is obtainable in the case of EIS experiments.

## EXPERIMENTAL PROCEDURES

The flat corrosion cell employed in this work is shown in Figure 1. Two 10.2- by 15.2-cm (4- by 6-in) 2219-T87 aluminum sheet specimens were anodized, one using the chromic acid technique (Type I per MIL-A-8625) and the other the standard sulfuric acid technique (Type II per MIL-A-8625). Both specimens were water sealed. Chemical analysis of the 2219-T87 aluminum alloy is shown in Table 1. Careful control of the plating operation produced a coating thickness of 15.2 microns (0.6 mil) on both specimens as measured with a micrometer. Cross-sectioning of the specimens after exposure revealed coating thicknesses of 13 microns (0.5 mil) for the chromic acid anodized specimen and 15 microns (0.6 mil) for the sulfuric acid anodized specimen. The two specimens, therefore, had comparable coating thicknesses which eliminated this variable as a factor in establishing differences in corrosion protection.

The sheet specimens were sanded on the back side to provide electrical contact. The front, anodized sides were cleaned with alcohol to remove fingerprints. They were then clamped into the corrosion cells and exposed to a corrosive medium of 3.5-percent sodium chloride (Na-Cl) solution at pH 5.5. Corrosion data were obtained for a period of 27 days, with EIS and PR data being obtained on alternate days for each sample. Silver/silver chloride reference electrodes were used in each case.

The EG&G-PARC model 378 ac impedance system was used for all corrosion measurements. For the EIS measurements, data were taken in three sections. The first two sections, beginning at 0.001 Hz and 0.1 Hz, respectively, were obtained using the fast Fourier transform technique. The last section, ranging from 6.28 to 40,000 Hz, was collected using the lock-in amplifier technique. The sequencing was performed automatically using the autoexecute procedure, with all data merged to a single set for each run. After collection, the data were processed and analyzed with an IBM PC/AT computer using the models of Figures 2 and 3. The same computer also controlled the experiment.



Data for the PR technique were collected using the same instrumentation with the EG&G-PARC model 342C software, which was developed especially for dc measurements. Instrumentation developed by EG&G-PARC automatically corrected the data for the IR drop during the scan. The potential applied to the specimen, during the scan, was varied from -20 mV to +20 mV on either side of the corrosion potential  $E_{\text{CORR}}$ , with data points (current and potential) being recorded in 1/4-mV increments. The data were processed and analyzed using the program POLCURR.<sup>8</sup> For this least-squares analysis, data points at 1.0-mV intervals were selected by the computer program. Values for the polarization resistance,  $I_{\text{CORR}}$ ,  $E_{\text{CORR}}$ , and the Tafel constants ( $b_a$  and  $b_c$ ) were thus obtained.

## RESULTS AND DISCUSSION

Curves for the charge transfer resistance at the metal-coating interface  $R(T)$ , the pore or coating resistance  $R(P)$ , and the Warburg coefficient  $\sigma$  versus time for the 2219-T87 aluminum alloy specimen anodized with the sulfuric acid technique are shown in Figure 4. Curves for the charge transfer resistance at the coating-solution interface  $R(F)$ , the solution resistance  $R(S)$ , and the corrosion current  $I_{\text{CORR}}$  versus time are shown in Figure 5. All  $I_{\text{CORR}}$ -time curves are those derived from PR measurements, while all other curves are the result of EIS measurements. Curves for values of the capacitors are not shown, but these all increased with time, consistent with a general decrease in impedance.

### Sulfuric Acid Anodize

For the specimen anodized in sulfuric acid, the charge transfer resistance at the metal-coating interface (Fig. 4a) oscillated to rather high values and approached a plateau at lower values after about 17 days. The pore resistance-time curve (Fig. 4b) gradually decreased during the entire test period, while the Warburg coefficient-time curve (Fig. 4c) approached a plateau at lower values after about 14 days. The curve for the charge transfer resistance at the coating-solution interface (Fig. 5a) oscillated, but seemed to stabilize at a lower value after about 23 days, while the curve for the solution resistance (Fig. 5b) generally decreased in value. The curve for  $I_{\text{CORR}}$  versus time (Fig. 5c) showed a generally gradual increase in value up to about 18 days, but increased rather rapidly to a maximum at about 24 days.

### Chromic Acid Anodize

The charge transfer resistance curve at the metal coating interface (Fig. 6a) for the specimen anodized in chromic acid dropped rather suddenly after about 4 days and gradually decreased with oscillation thereafter. Curves for the pore resistance (Fig. 6b) and the Warburg coefficient (Fig. 6c) decreased with oscillation, dropping to rather low values after about 24 days. The charge transfer resistance curve for the coating-solution interface (Fig. 7a) decreased gradually for about 24 days, but showed a rapid rise at the end of that time. The  $I_{\text{CORR}}$ -time curve (Fig. 7c) increased gradually with oscillation for almost the entire period, but increased rapidly after 24 days.

### Comparison of Charge Transfer Resistance, Pore Resistance, and Diffusion Coefficients

Values for the charge transfer resistance at the metal-coating interface are generally much higher for the sulfuric acid anodize than for the chromic acid anodize. Values for the pore resistances are

comparable in both cases. Values for the Warburg or diffusion coefficients are also much higher for the sulfuric acid anodize, indicating that diffusion of the electrolyte through the coating is less pronounced in the sulfuric acid anodize case. Also, values of the charge transfer resistance at the metal-coating interfaces are much larger than values for the Warburg coefficients in both cases, indicating that the corrosion kinetics are charge transfer controlled.

### **Corrosion Rates**

Values of the corrosion rates for the chromic acid anodize and the sulfuric acid anodize, obtained by both the EIS and PR methods, are listed in Table 2. Values for the Tafel constants in the EIS method are assumed, while they are obtained as part of the experimental data in the PR method. Both the average corrosion rates for the first 7 days and those for the entire 27-day period are shown, together with the percent increase of those for the 27-day period over those of the 7-day period. From the results, it is clear that Type II sulfuric acid anodizing offers corrosion protection superior to that by Type I chromic acid anodizing, and elimination of the chromic acid method should pose no problem as far as corrosion protection is concerned.

### **CONCLUSION**

The results of this study indicate that Type II sulfuric acid anodizing is superior to Type I chromic acid anodizing as far as the corrosion protection of aluminum is concerned. Therefore, the elimination of chromic acid anodizing to conform with federal and state mandates restricting the use of hexavalent chromium should present no problem in this regard.

## REFERENCES

1. Danford, M.D.: NASA Technical Memorandum, NASA TM-100402, June 1990.
2. Busing, W.R., and Levy, H.A.: "A General Nonlinear Least Squares Program ORGLS." Oak Ridge National Laboratory, 1958.
3. Stern, M., and Geary, A.L.: Journal of the Electrochemical Society, vol. 102, 1955, p. 609.
4. Stern, M., and Geary, A.L.: Journal of the Electrochemical Society, vol. 104, 1957, p. 56.
5. Stern, M.: Corrosion, vol. 14, 1958, p. 440t.
6. Danford, M.D.: NASA Technical Memorandum, NASA TM-100366, April 1989.
7. Gerchakov, S.M., Udey, L.R., and Mansfeld, F.: "An Improved Method for Analysis of Polarization Resistance Data." Corrosion, vol. 37, 1981, p. 696.
8. Danford, M.D., and Higgins, R.H.: NASA Technical Paper 2459, April 1985.

**Table 1**  
**Chemistry of 2219-T87 Aluminum.**

<u>Element</u>	<u>Listed Weight Percent</u> <u>(ASTM B-209)</u>	<u>Measured Weight Percent</u> <u>(MSFC Analysis)</u>
Silicon	0.2 Maximum	0.100
Copper	5.8 – 6.8	6.700
Iron	0.3 Maximum	0.227
Manganese	0.2 – 0.4	0.220
Zinc	0.1 Maximum	0.030
Titanium	0.02 – 0.10	0.085
Vanadium	0.05 – 0.15	0.092
Zirconium	0.10 – 0.25	0.128
Chromium	0.05 Maximum	0.024
Aluminum	Balance	92.394

**Table 2**  
**Comparison of Average Corrosion Rates Obtained With AC and DC Methods.**

<u>Method</u>	<u>EIS*</u> <u>7 Days</u> <u>mpy</u>	<u>PR†</u> <u>7 Days</u> <u>mpy</u>	<u>EIS*</u> <u>27 Days</u> <u>mpy</u>	<u>Percent</u> <u>Increase</u>	<u>PR†</u> <u>27 Days</u> <u>mpy</u>	<u>Percent</u> <u>Increase</u>
Chromic Acid	0.03536	0.02513	0.09602	171.5	0.06540	160.2
Sulfuric Acid	0.01213	0.00957	0.01790	47.5	0.01152	20.4

\* Electrochemical impedance spectroscopy (ac).

† Polarization resistance technique (dc).

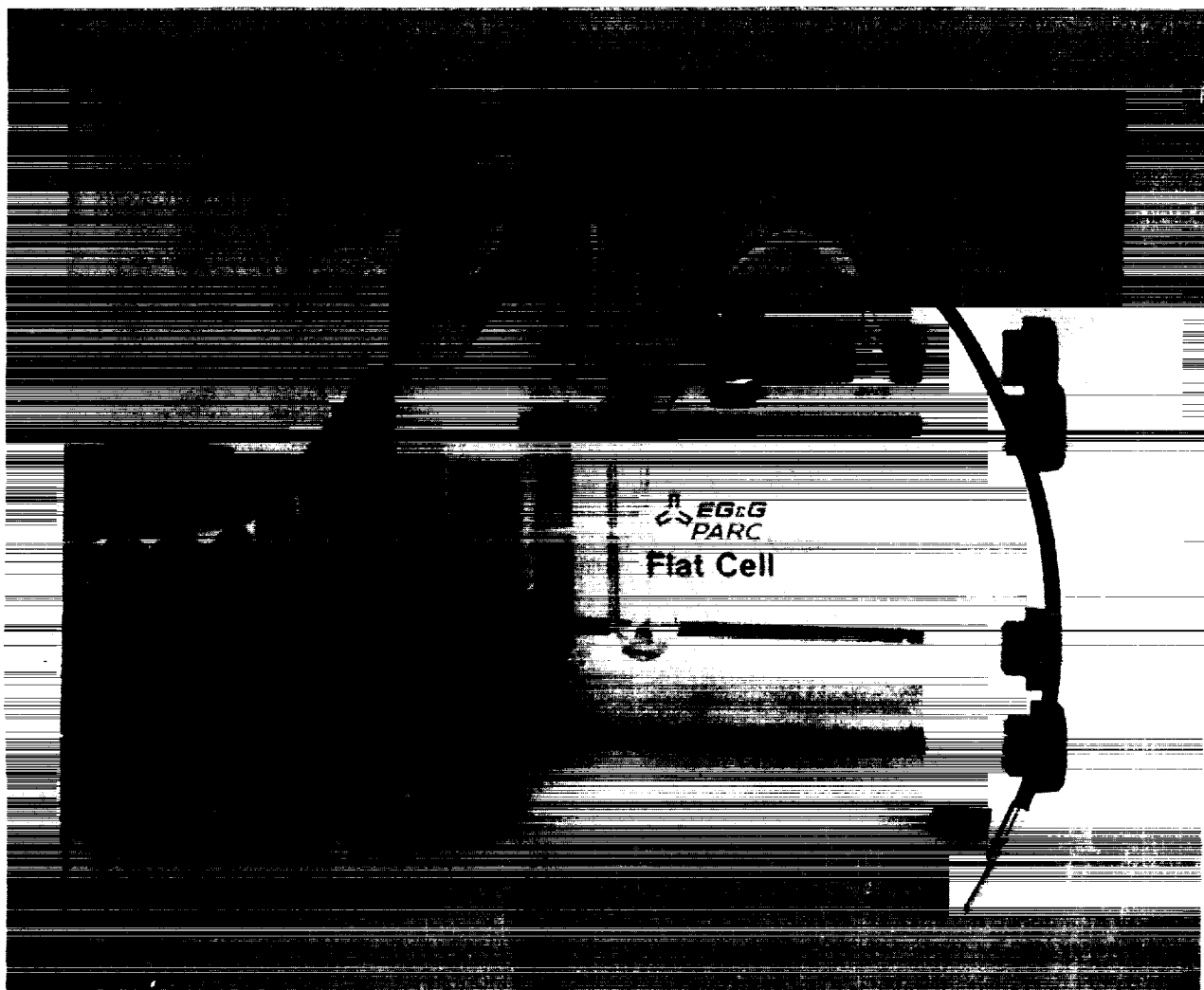
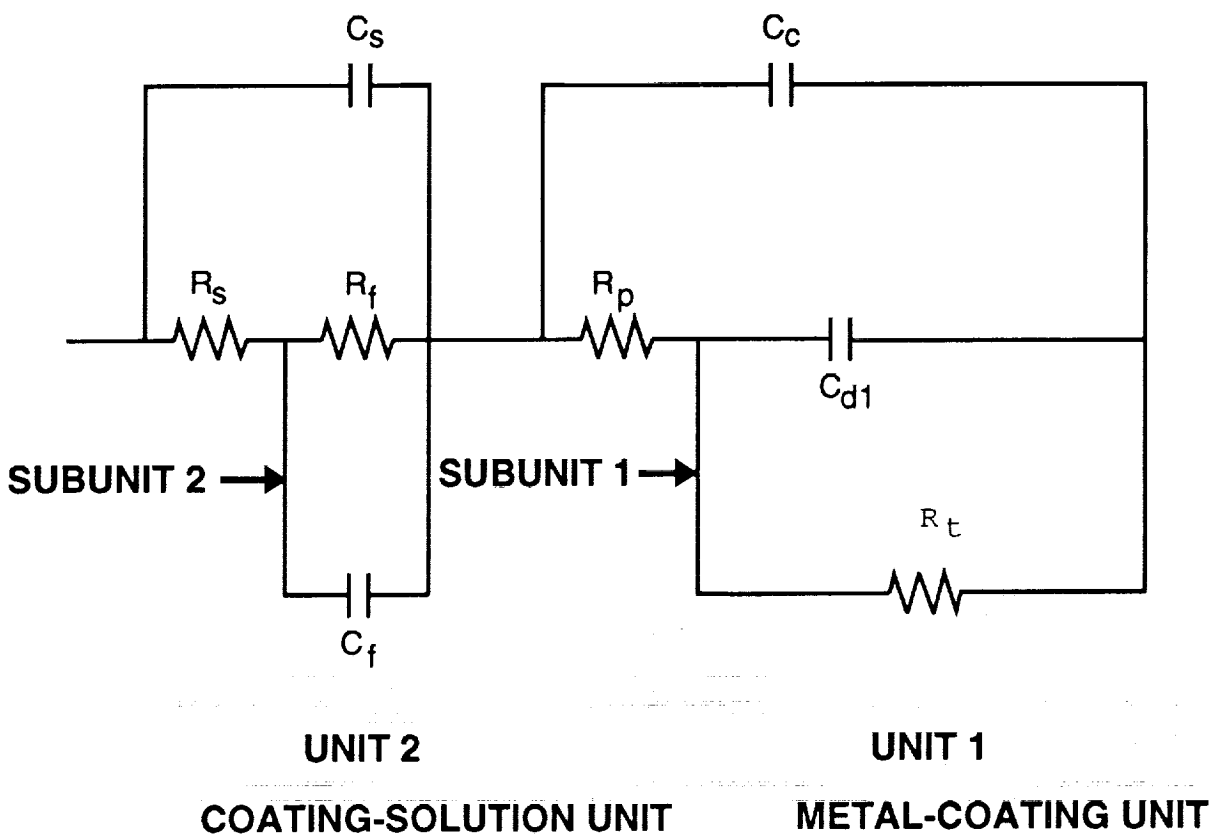


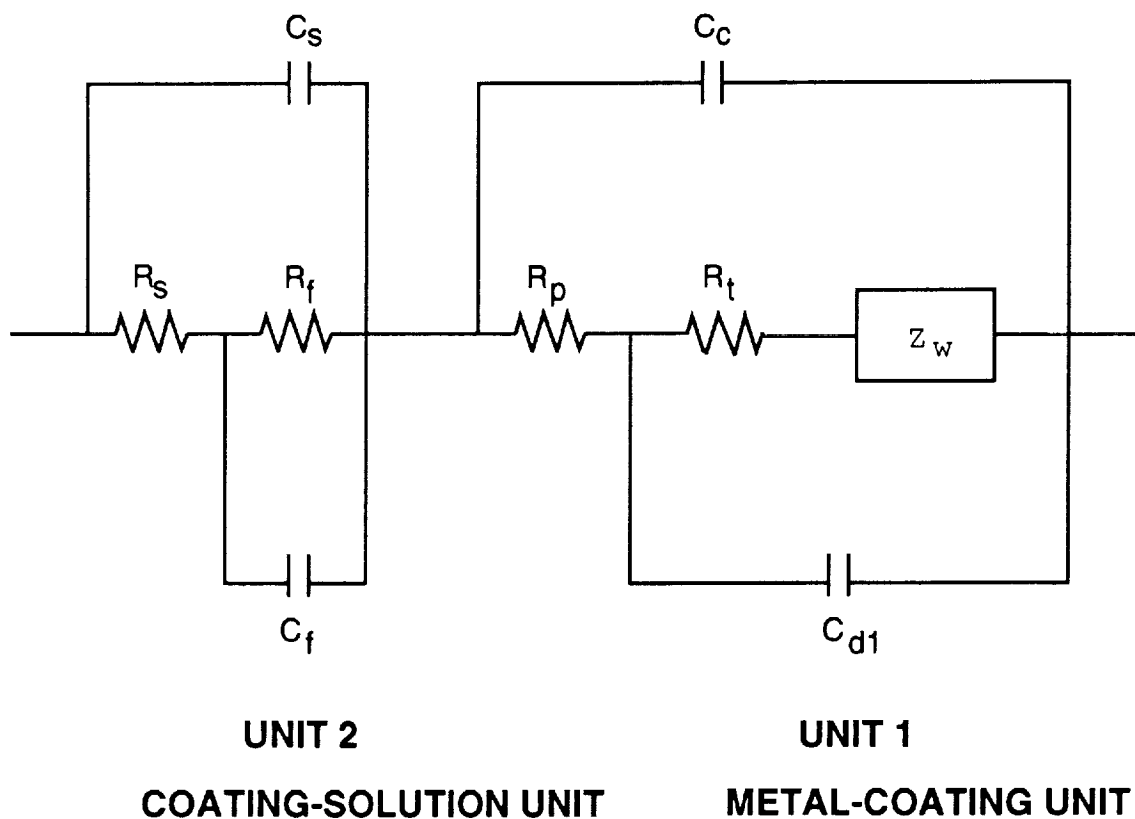
Figure 1. The New EG&G-PARC Flat Cell.

ORIGINAL PAGE  
BLACK AND WHITE PHOTOGRAPH



- $C_s$  SOLUTION CAPACITANCE
- $R_s$  SOLUTION RESISTANCE
- $C_f$  FARADAIC CAPACITANCE (COATING/SOLUTION)
- $R_f$  FARADAIC RESISTANCE
- $C_c$  COATING CAPACITANCE
- $R_p$  COATING RESISTANCE
- $R_t$  CHARGE TRANSFER RESISTANCE
- $C_{d1}$  METAL/COATING INTERFACE CAPACITANCE

Figure 2. Primary Equivalent Circuit Model for Analysis of AC Impedance Data.



- $C_s$  SOLUTION CAPACITANCE
- $R_s$  SOLUTION RESISTANCE
- $C_f$  FARADAIC CAPACITANCE (COATING/SOLUTION)
- $R_f$  FARADAIC RESISTANCE
- $C_c$  COATING CAPACITANCE
- $R_p$  COATING RESISTANCE
- $R_t$  CHARGE TRANSFER RESISTANCE
- $C_{d1}$  METAL/COATING INTERFACE CAPACITANCE
- $Z_w$  WARBURG IMPEDANCE (DIFFUSION POLARIZATION)

Figure 3. Equivalent Circuit Model for Calculating the Warburg Coefficient.

## Sulfuric Acid Anodize

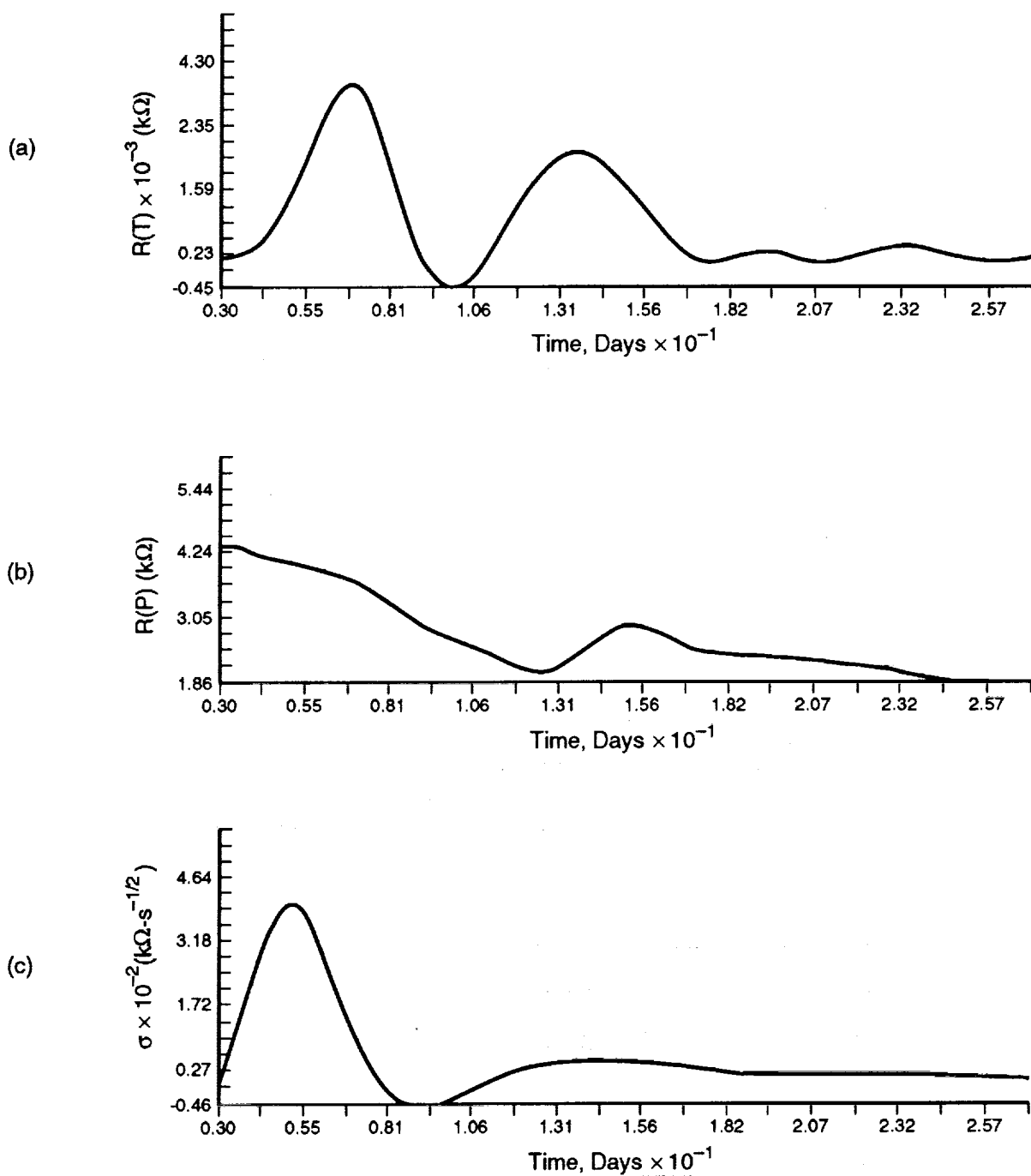


Figure 4.  $R(T)$ ,  $R(P)$ , and  $\sigma$ -Time Curves for Sulfuric Acid Anodize.



## Sulfuric Acid Anodize

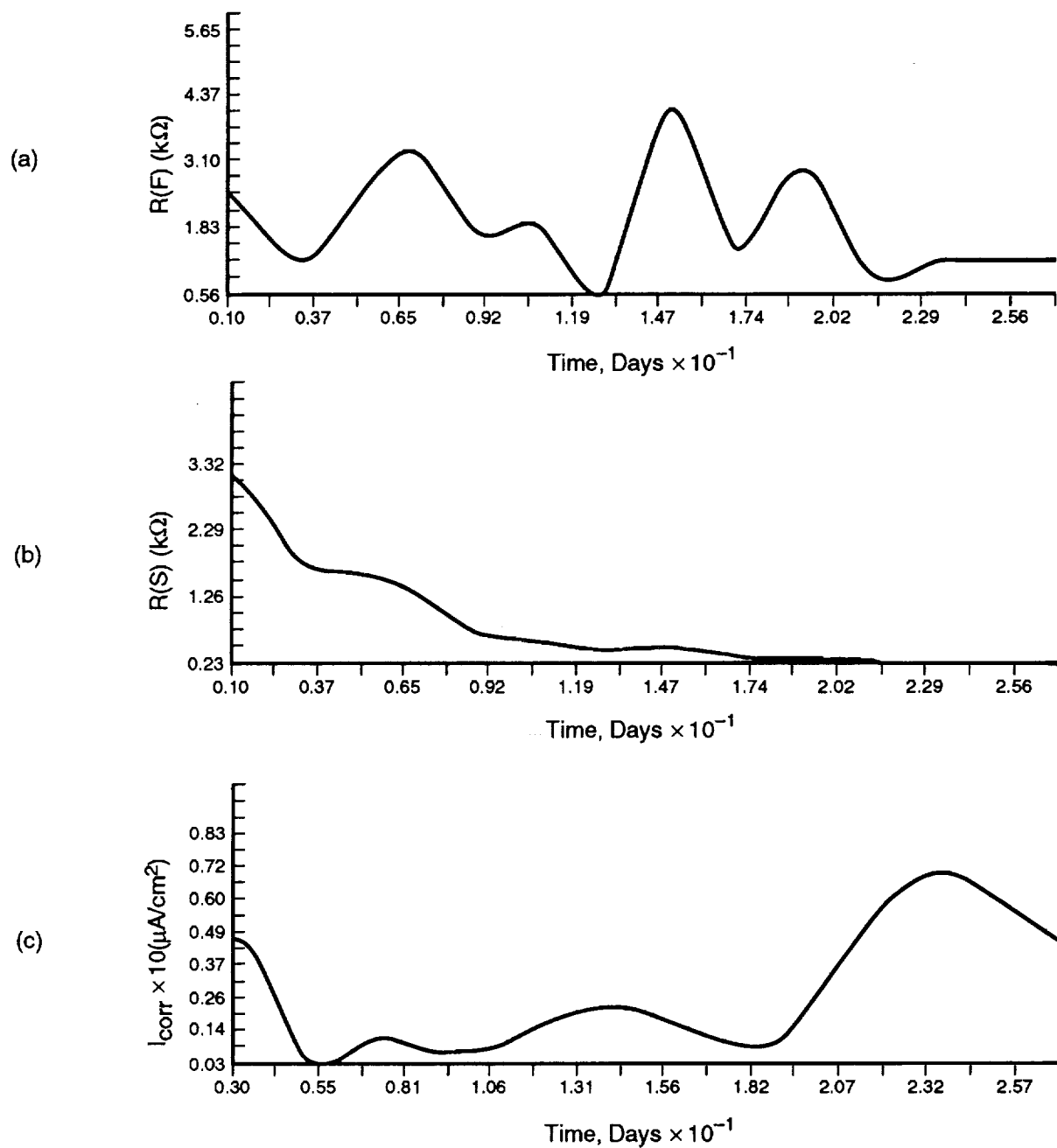


Figure 5.  $R(F)$ ,  $R(S)$ , and  $I_{CORR}$ -Time Curves for Sulfuric Acid Anodize.

## Chromic Acid Anodize

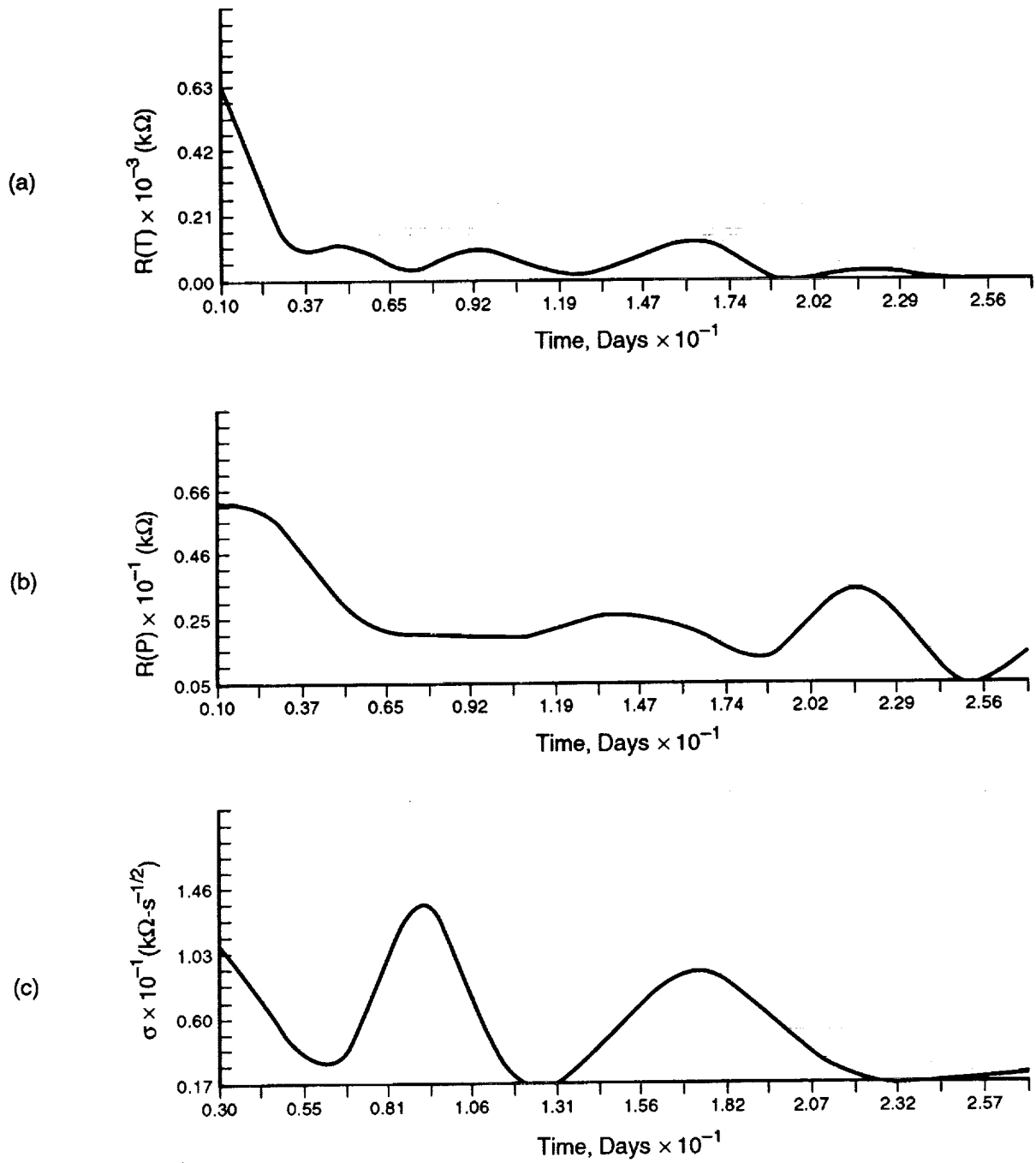


Figure 6.  $R(T)$ ,  $R(P)$ , and  $\sigma$ -Time Curves for Chromic Acid Anodize.

## Chromic Acid Anodize

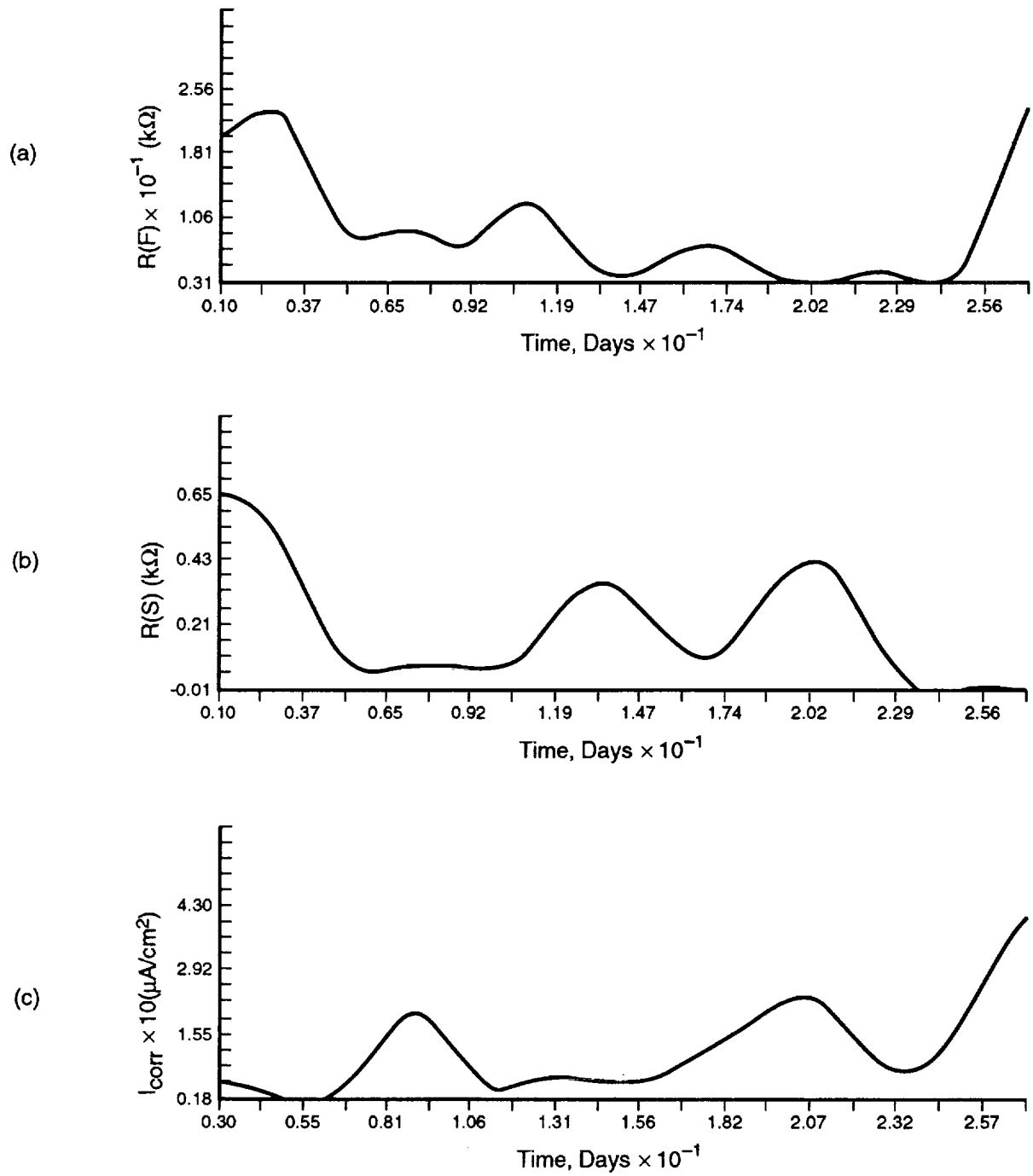


Figure 7.  $R(F)$ ,  $R(S)$ , and  $I_{\text{CORR}}$ -Time Curves for Chromic Acid Anodize.



APPROVAL

A COMPARISON OF CHROMIC ACID AND SULFURIC ACID ANODIZING

By M. D. DANFORD

The information in this report has been reviewed for technical content. Review of any information concerning Department of Defense or nuclear energy activities or programs has been made by the MSFC Security Classification Officer. This report, in its entirety, has been determined to be unclassified.

*J. W. Montano 8/27/92*  
\_\_\_\_\_  
J. W. Montano  
Chief  
Corrosion Research Branch

*Paul M. Munafo 9/8/92*  
\_\_\_\_\_  
Paul M. Munafo  
Chief  
Metallic Materials Division

*Paul H. Schuerer 9/8/92*  
\_\_\_\_\_  
Paul H. Schuerer  
Director  
Materials & Processes Laboratory

